# Coated grains in the Upper Cretaceous Ilam Formation: implication for paleoclimatic reconstruction

**Amirhossein Enayati-Bidgoli[1]*, Hossain Rahimpour-Bonab[2], Amin Navidtalab[3]**
[1] *Department of Petroleum Geology, Research Institute of Petroleum Industry (RIPI) 14857-33111 Tehran, Iran*
[2] *School of Geology, College of Science, University of Tehran, 14176-14411 Tehran, Iran*
[3] *School of Earth Sciences, Damghan University, 36716-41167 Damghan, Iran*
**Corresponding author, e–mail: amirhossein.enayati@gmail.com*
(*received: 13/07/2019 ; accepted: 07/12/2019*)

**Abstract**

The Upper Cretaceous Ilam carbonate Formation has been analyzed for its coated grains (fine ooids and rhodoids) in oilfields of SW Iran. The recognized coated grains are morphologically classified into several types. Petrographic and geochemical characteristics indicate that the ooids were originally composed of low-magnesium calcite (LMC; consistent with global observations), but rhodoids consisted originally of high-magnesium calcite (HMC). The overall primary mineralogy of the intervals containing coated grains has been a mixture of HMC and LMC. Co-occurrence of these mineralogies and allochemical (both ooids and rhodoids and other bioclasts) components indicates a rhodalgal-like grain association and a relatively temperate paleoclimatic conditions.

**Keywords**: *Coated Grains, Ooid, Rhodoid, Ilam Formation, Upper Cretaceous.*

## Introduction

In marine carbonates, grain types are paleoenvironmental proxies for water energy level, sedimentation rate, depositional setting, and sea-level fluctuation; and they provide significant insights into the global secular variations of carbonate mineralogy in Phanerozoic oceans (e.g. Stanley & Hardie, 1998). Carbonate grain associations and compositions can be used to reconstruct paleoclimatic and paleolatitudinal zones. They are and also served to detect cyclic sedimentation and sequence stratigraphic positions. For example, ooids as a product of marine water physicochemical processes could be used for evaluating atmospheric–hydrospheric paleochemical variations throughout the Phanerozoic (Wilkinson *et al*., 1983). Moreover, grain type, mineralogy, and spatial variation of grains can be major controls over the porosity development in reservoir rocks (Flügel, 2010).

Throughout the Arabian Platform and Zagros fold-thrust belt (Figs. 1a to 1c), the Cretaceous successions host considerable amounts of the world's total hydrocarbon reserves (Setudehnia, 1978; Scott *et al*., 1993; Al-Sharhan & Nairn, 1993; Hollis, 2011). Compared to the most periods of the Phanerozoic, coated grains show a unique occurrence in the late Cretaceous aged Ilam Formation and its counterparts (Figs. 1d and 2; Rahimpour-Bonab *et al*., 2013; Navidtalab *et al*., 2016). Coated grains are uncommon in the global, late Cretaceous aged successions (Wilkinson *et al*., 1985).

Among the stratigraphic equivalents of the Ilam Formation in the Arabian Plate (Ilam in Dubai region, UAE and northern Oman Mountains [Schlumberger, 1981; Alsharhan & Kendall, 1995; Alsharhan & Nairn, 2003]; Muti in the northern UAE [Alsharhan, 1989]; Halul in Qatar [Sugden & Standring, 1975]; Sa'di in Kuwait [Alsharhan & Nairn, 2003]; Kometan in the central and northern Iraq [Bellen *et al*., 1959]; Fiqa in Oman Foredeep Basin [Tschopp, 1967a,b; Wilson, 1969; Glennie *et al*., 1974]; Wadi Umm Ghudran and Hamza formations in Jordan [Alsharhan & Nairn, 2003]; Soukhne in Syria [Alsharhan & Nairn, 2003]; Karababa in southeast Turkey [Rigo & Cortesini, 1964; Cater & Gillcrist, 1994]; and probably the Tanuma Formation in the southern Iraq), only the Tanuma Formation in the southern Iraq contains an oolitic bed at its top (Owen & Nasr, 1958; Bellen *et al*., 1959). Facies analysis in the Izeh Zone (Zagros Area; Fig. 1c) indicates that the Ilam carbonates contain ooids (Adabi & Asadi-Mehmandosti, 2008), but their stratigraphic distribution or positions were not illustrated. Moreover, in the Zagros Thrust Zone (Bangestan anticline; Fig. 1c), ooid bearing facies of the Ilam Formation were recognized (Ghabeishavi *et al*., 2009). Additionally, in the study area (Dezful Embayment), considerable deposition of the coated grains is observed in the Ilam Formation. They were deposited during a transitional period from a very warm (middle Cretaceous) to a relatively cool (late Cretaceous) climates (Douglas & Savin, 1973, 1975; Arthur *et* *al*., 1985; Barrera *et al*., 1987; Barrera *et al*., 1997; Spicer & Corfield, 1992; D'Hondt & Lindinger, 1994; Huber *et al*., 1995; D'Hondt & Arthur, 1996; Li & Keller, 1998a, b). This coincides with the global increase of calcitic ooids during the Cretaceous time (Mackenzie & Agegian, 1989). Therefore, it is attempted to evaluate the paleoclimatic conditions associated with paleolatitudinal zones using coated grain associations and compositions in the study area.

## Geological setting, paleogeography, and stratigraphy

Paleogeographic studies of the Cretaceous successions in the Middle East suggested that during this period the Arabian plate was located at the 10–15º N latitudes (tropical and subtropical; Figs. 1a and 1b; Murris, 1980; Beydoun, 1991; Beydoun *et al*., 1992; Sharland *et al*., 2001; Alavi, 2004, 2007; Heydari, 2008).

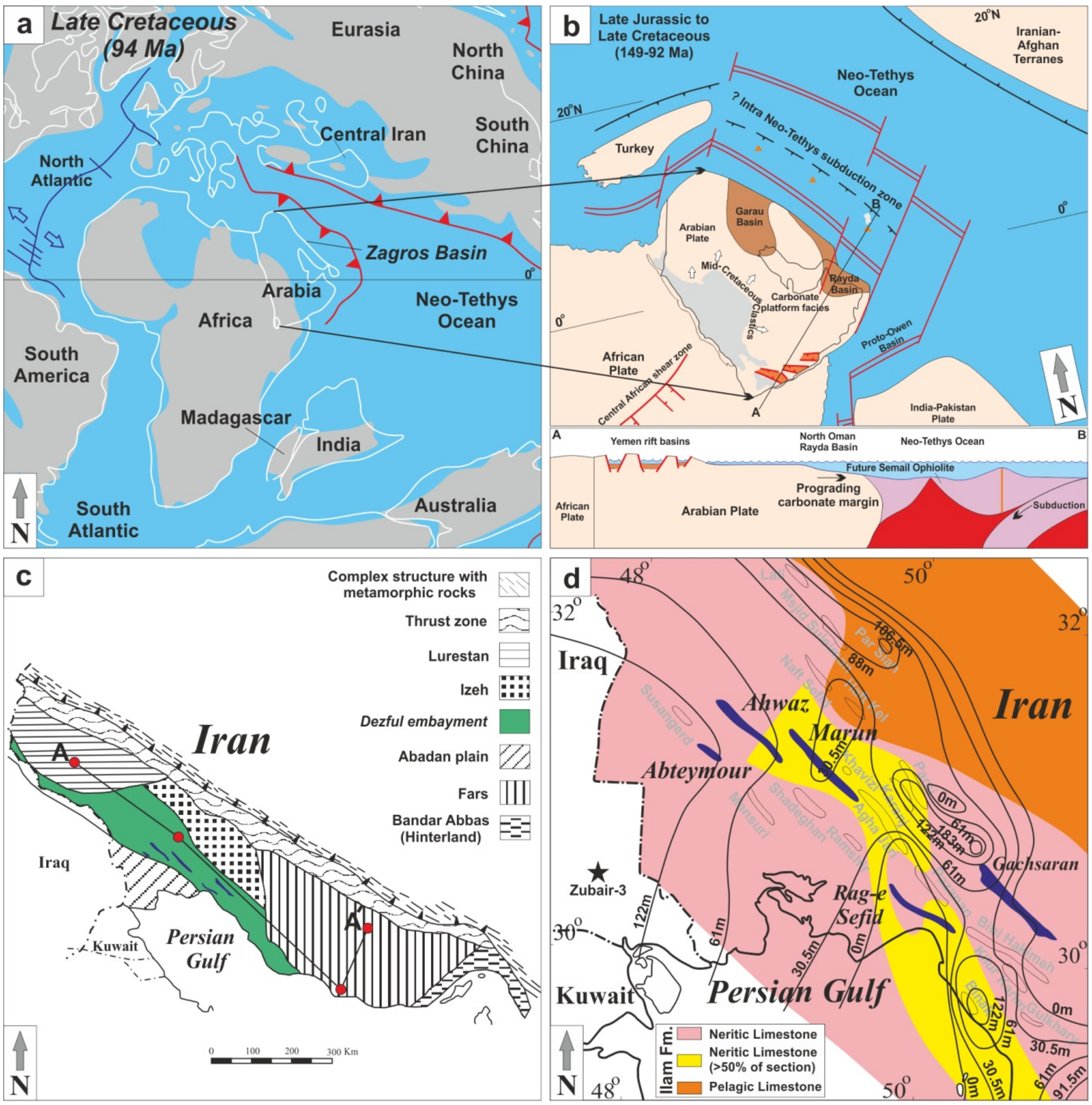


Figure 1. a: Paleogeographic position of the studied area (SW Iran) during the Late Cretaceous (modified from http://paleoportal.org). b: Tectonic setting and paleogeographic location of the Arabian Plate and SW Iran during the Late Jurassic–Late Cretaceous time (Sharland *et al*., 2001). c: Structural subdivisions of the Zagros region (Aghanabati, 2004) and the location of five studied fields in the Dezful Embayment subdivision (see Fig. 2 for A–A′ cross section). d: Location of five studied fields (dark blue color), isopach map, paleogeography, and lateral facies changes of the Ilam Formation in the studied area (compiled from Hart, 1970; Khalili, 1974).

In this time, ramp-type depositional settings associated with shelf carbonates were established and gradually dominated most parts of this area due to the eustatic sea-level rise (Murris, 1980; Koop & Stoneley, 1982). The global relative sea-level curve (first order) shows that the Cretaceous Bangestan carbonates (e.g. the Ilam Formation) were deposited during a global highstand and highest relative sea level during the Phanerozoic (Vail *et al*., 1977).

During the Late Cretaceous and later, the occurrence of several paleo-structures as a result of the Neo-Tethys subduction beneath the Central Iran, and the ophiolite obduction on the NE margin of the Arabian Plate (Figs. 1a to c; Hart, 1970a; Sepehr & Cosgrove, 2004; van Buchem *et al*., 2011; Hollis, 2011; Casini *et al*., 2011; Mehrabi & Rahimpour-Bonab, 2014; Navidtalab *et al*., 2016; Navidtalab *et al*., 2019) led to important lateral changes in the sedimentological, paleontological and geochemical characteristics of synchronous carbonate deposits (Sepehr & Cosgrove, 2004; Alavi, 2004, 2007; Rahimpour-Bonab *et al*., 2012a; Rahimpour-Bonab *et al*., 2013). Consequently, carbonate sequences of this time interval (i.e. the Ilam Formation) show variable sedimentological characteristics across the Zagros, especially in the Dezful Embayment (Fig. 2).

The Albian–Campanian aged Bangestan Group (Fig. 2) hosts some of the most prolific reservoirs in the hydrocarbon provinces of the Arabian Platform and Zagros fold-thrust belt (Motiei, 1993; Aqrawi *et al*., 1998; Rahimpour-Bonab *et al*., 2012a, b). The most important interval of this group includes the Sarvak and Ilam formations which provides reservoir for many giant and supergiant oilfields such as the fields from the southern Dezful Embayment including the Abteymour, Ahwaz, Marun, Gachsaran, and Rag-e Sefid (Figs. 1c and d).

The Ilam Formation (the upper part of the Bangestan group; Fig. 2) consists of both shallow-water and deeper-water sediments (Figs. 1d and 2). Deeper-water facies prevails in Lurestan, but the Khuzestan (the studied area) and Fars may exhibit both or either of facies (James & Wynd, 1965; Figs. 1d and 2). However, in most parts of the SW Iran, including the Dezful Embayment, the Ilam Formation is generally represented by the shallow water limestones that unconformably overlies the carbonates of the Sarvak Formation (Navidtalab *et al*., 2016), and is conformably overlain by shales and marls of the Gurpi Formation (e.g. James & Wynd, 1965; Fig. 2).

## Materials and methods

The data sets used for this study are obtained from six wells drilled in the Abteymour (AT-1), Ahwaz (AZ-1), Marun (MN-1), Gachsaran (GS-1 and GS-2), and Rag-e Sefid (RS-1) oilfields that located in the Dezful Embayment, SW Iran (see Rahimpour-Bonab *et al*., 2013 for more details; Fig. 1d).

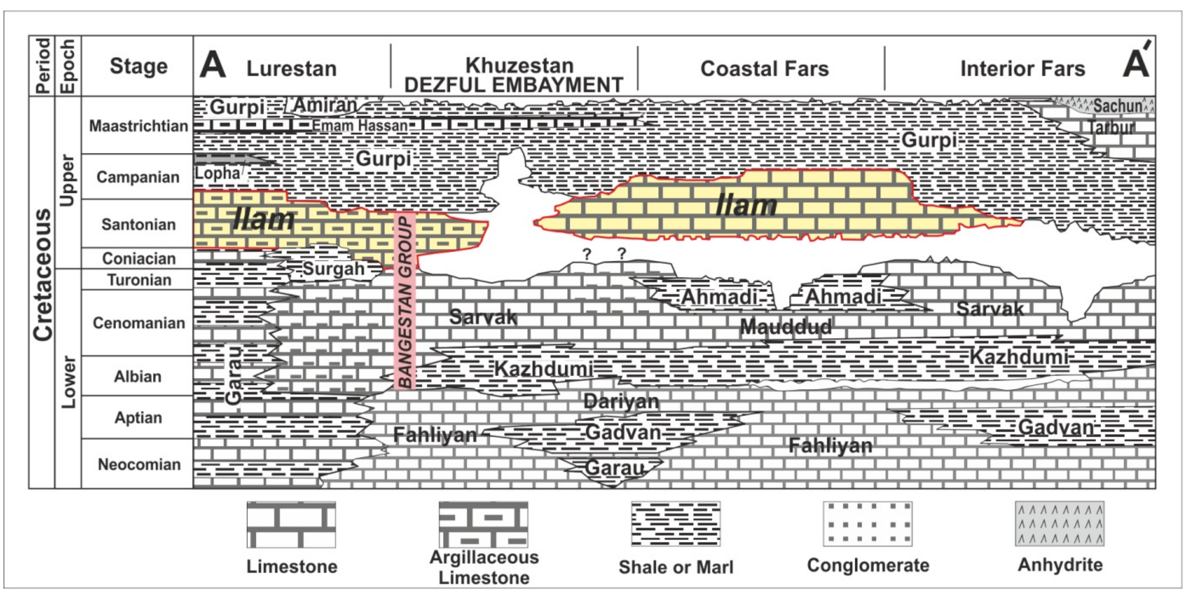


Figure 2. Stratigraphic correlation chart of the Cretaceous formations throughout the Zagros (A–A′ cross section; see Fig. 1) and also lateral extension of the studied Ilam Formation (compiled from James & Wynd, 1965; Christian, 1997).

To investigate the Ilam Formation in the Abteymour (AT-1), Ahwaz (AZ-1), and Marun (MN-1) oilfields, about 200 m of cores were examined. Petrographic analyses (almost 250 thin sections with 0.25 to 1 m spacing) along with image and quantitative analyses of all components were applied to determine the facies variations and the diagenetic features of the Ilam carbonates. For microfacies descriptions and facies analysis, standard models are considered (e.g. Wilson, 1975; Buxton & Pedley, 1989; Pedley, 1998; Flügel 2004) that are described in details in Mehrabi *et al.* (2014).

Due to the absence of appropriate bioclasts in the studied successions, bulk samples were used for the stable isotopes and trace element analyses. To avoid stylolites and filled microfractures as the only visible secondary/diagenetic features during the sampling thin sections and core samples were examined using polarizing and binocular microscopes. A 0.5 mm tungsten carbide bit was used for drilling and sampling. A total of 62 and 63 samples were analyzed for trace elements and for oxygen and carbon stable isotopes, respectively. Oxygen and carbon stable isotope analyses were carried out at Texas A&M University using a Gas Bench online with a Finnigan Delta-Plus XP. The $\delta$ values are presented with reference to the PDB standard in permil (‰). For elemental concentrations, powdered samples were reacted with nitric acid ($HNO_3$) to remove organic compounds, and hydrochloric acid (HCl) to comprise carbonate phase. Then, they were diluted with distilled water, and finally, analyzed by PerkinElmer AAnalyst 100 atomic absorption spectrometer for Ca, Sr, and Mn at the geochemistry laboratory, School of Geology, University of Tehran. The precision was ±5 ppm for Sr and Mn, and around 0.5 % for Ca.

All types of recognized coated grains are described according to their overall shape, shape and thickness of cortex, type and size of nucleus, cortex microfabrics (concentric vs. radial), and number / thickness of lamellas. Following the description of all detectable coated grains, detailed petrographic (diagenesis) and geochemical analyses are considered to detect the primary mineralogy of the coated grains as a proxy for the paleoenvironmental reconstruction. The main aim of this study is to describe and elaborate the environmental factors triggering the occurrence of these allochems.

## Results

In the studied wells, the occurrence of coated grains was confined to the upper parts of the Ilam Formation (Fig. 3). Two main groups of coated grains were recognized in thin sections including (micro-) ooids and rhodoids (Figs. 4 and 5). These coated grains show variations in the studied wells in terms of their frequency, concomitant allochemical components, and their stratigraphic location (Fig. 3). In these subsurface sections, rhodoids are more frequent than ooids (Figs. 1d and 3). The highest thickness of the Ilam Formation and also coated grain bearing intervals are in the Abteymour oilfield (AT-1). There is no evidence of oolitic intervals in the AZ-1 well. Generally, oolitic units are observed as thin layers in the AT-1 and MN-1 wells. Coated grain bearing intervals or upper part of the Ilam Formation can be considered as a highstand systems tract.

Geochemical data are presented in Figure 6. The Sr content of the analyzed samples (with and without coated grains) varies between 350 and 750 ppm with an average of 572 ppm. Mn content ranges from 70 to 630 ppm with an average of 218 ppm. Ca concentrations of the samples vary between 16 % and 41 % with an average of 27 %. $\delta^{13}C$ varies mostly between 1 and 3.5 ‰, except for two samples with low values of −0.2 and −3.5 ‰ in AT-1 and MN-1 at depths 3127.55 m and 3613 m, respectively. $\delta^{18}O$ of samples ranges from −1.5 to −5.5 ‰. Stratigraphic variation of the geochemical data is represented by Figure 6 which does not show differentiation with respect to the facies association.

## Coated grains

Coated grains are only visible in three oilfields from the Dezful Embayment. Those are mostly composed shallow marine facies (Fig. 3). The recognized coated grains include two main groups including (fine-) ooids and rhodoids that are morphologically subdivided into several types.

## Ooids group

The recognized ooids are subdivided into three types including superficial, concentric-radial and compound ooids. Ooids are detected as thin intervals in the Ilam Formation, represented by ooid grainstones (Fig. 3).

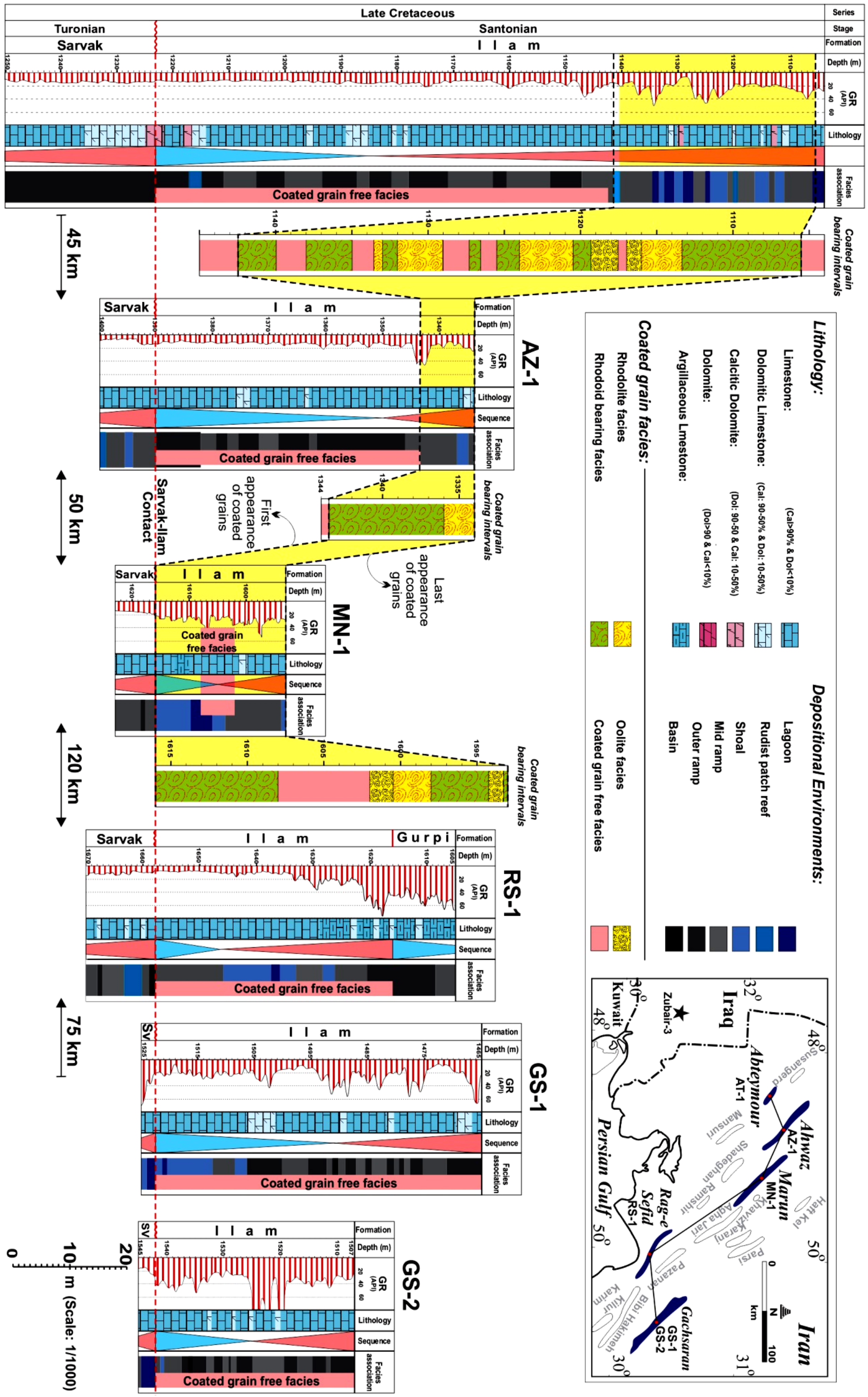


Figure 3. Correlation of coated grain bearing intervals of the Ilam Formation between wells of the studied fields.

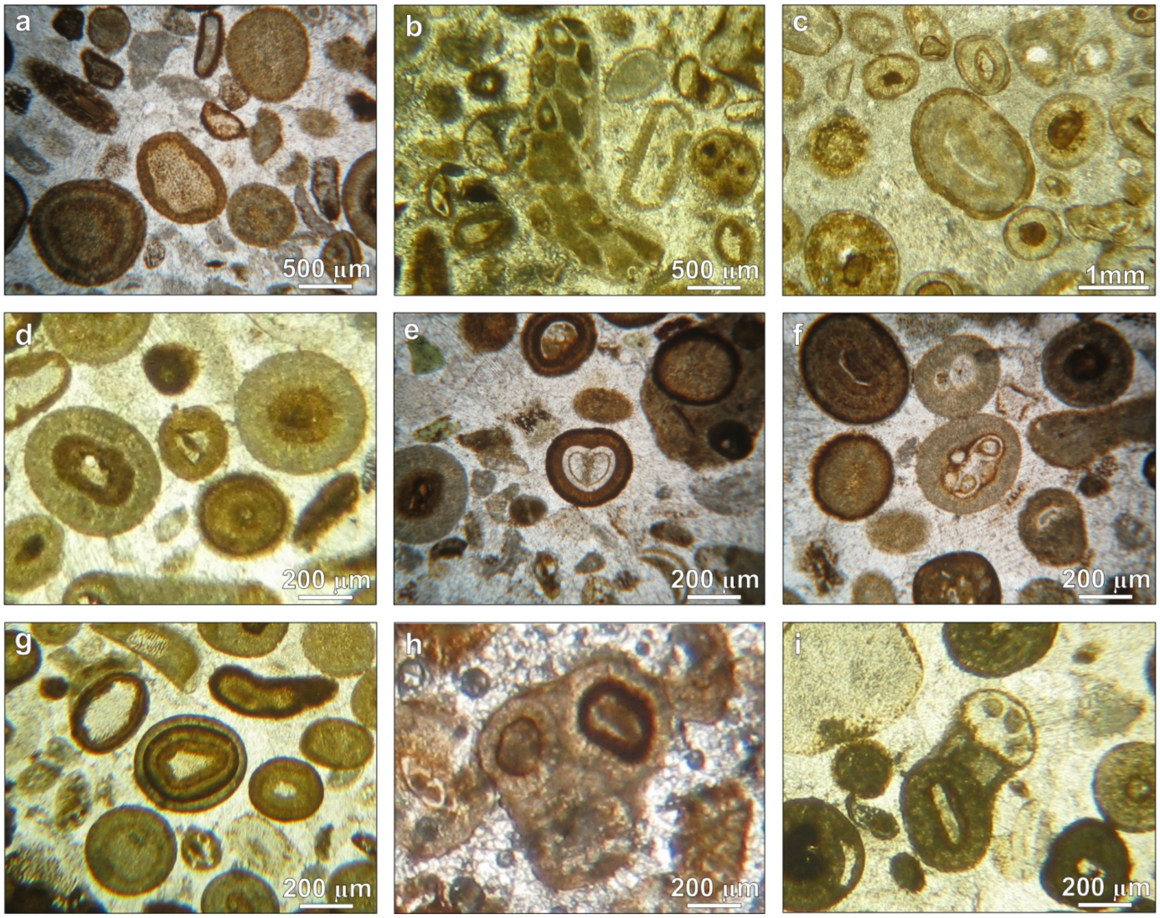


Figure 4. Ooid types in the Ilam Formation: a–b Superficial; c–g Concentric-radial; h–i Compound.

The ooid grainstones are present in two intervals with 1 and 2 m thicknesses in well AT-1. A 2 m thick unit in also observed in well MN-1 (Fig. 3). The main characteristics of recognized ooid types are as follows:

1. Superficial ooids:This type of ooids has a large nucleus and a thin concentric cortex with a few lamellas (Figs. 4a and 4b). The nuclei of the superficial ooids are mainly echinoderm or bryozoan debris that their shapes determined the ultimate form of ooids (Figs. 4a and 4b). The cortex thickness is less than the half of the ooid diameter. Most likely, this resulted from slower motion of larger nuclei compared to the smaller ones (Harris, 1979).

2. Concentric-radial ooids: In the studied section, the dominant ooids are fine (0.2 to 0.5 mm in diameter), honey colored, and concentric-radial types (Figs. 4d to 4g; Heller *et al*., 1980; Tucker 1984). In some cases, there are fully concentric types as a primary feature (Fig. 4c; Sandberg, 1975; Simone, 1981; Richter, 1983). Observations proved that a diameter of 0.6 mm marks the threshold between particles transported by suspension (radial) and bed load (concentric; Middleton, 1976; Miller *et al*., 1977; Heller *et al*., 1980).

The observed ooids have small nuclei such as small benthic foraminifera (Figs. 4e and 4f) and echinoderm/bivalve debris along with thick cortices—several tens of lamellas–which reflect the basic feature of high-energy ooids (Figs. 4c to 4g; Mei & Gao, 2012).

3. Compound ooids: This type of ooids is rare and appears as two or three (superficial) ooids enveloped by a thin cortex of several lamellas (Figs. 4h and 4i).

**Rhodoids group**

The recognized rhodoids are subdivided into five types based on their internal and external characteristics including overall shape, shape and thickness of cortex, type and size of nucleus, pattern of cortex accretion, and number/thickness of lamellae (Fig. 5) which are described hereafter.

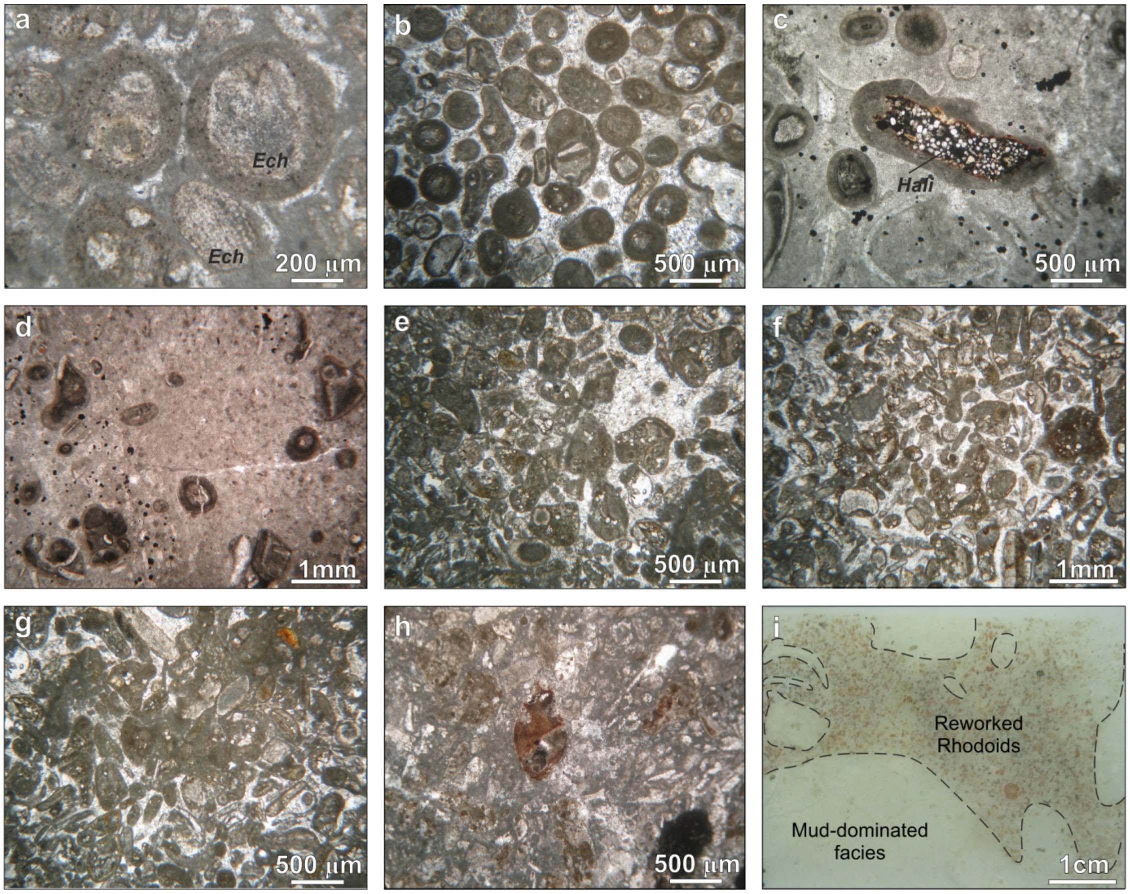


Figure 5. Rhodoid types in the Ilam Formation: a: Superficial (Ech=Echinoderm); b–d: Concentric (Hali=*Halimeda*); e–f: Compound; g: Loose; h-I: Reworked.

1. Superficial rhodoids: This type of rhodoids is common with large nucleus—compared to its cortex.The nuclei are mainly echinoderm fragments (Fig. 5a). The cortex is concentric with the thickness less than the half of the rhodoid diameter (Carozzi, 1957), and composed of several lamellae as a result of discontinuous coating (Fig. 5a). The average size is around 0.5 mm (Fig. 5a).

2. Concentric rhodoids: They are well rounded due to continuous rolling. They have small nuclei–compared to the overall size–which are echinoderm, bryozoan, bivalve and green algae (e.g. Halimeda) debris, and small benthic foraminifera (Figs. 5b to 5d). The concentric rhodoids are similar to superficial types but have smaller nuclei. Seemingly, there is an inverse relationship between the size of nucleous and thickness of cortex. Mainly, rhodoids with (large) echinoderm nuclei have a few lamellas (Figs. 5a and 5c vs. 5d). The cortex lamellas are concentric and vary from irregular to regular (Figs. 5b to 5d). The mean size of these rhodoids is 0.5 mm.

3. Compound rhodoids: This type of rhodoid is composed of two or more rhodoids which are bounded together via several lamellas, probably by encrusting algae (Figs. 5e and 5f). In comparison with single rhodoids (concentric and/or superficial), composite rhodoids are angular and larger than 0.5 mm (about 1 mm).

4. Amalgamated rhodoids: These rhodoids are amalgamated, and recognition of a single rhodoid is difficult (Fig. 5g). Usually the nuclei such as echinoderm fragments are recognizable. In some cases, the concentric structure of rhodoids is evident (Fig. 5g).

5. Reworked rhodoids: The main characteristics of this type are irregular shape, carved margins, stained appearance, and poor sorting (Figs. 5h and 5i). These are formed by reworking of older rhodoids. Facies containing these allochems display turbulence features such as facies heterogeneity (Fig. 5i) and Fe-oxide staining which are possibly related to non-deposition periods or sediment starvation (Flügel, 2010).

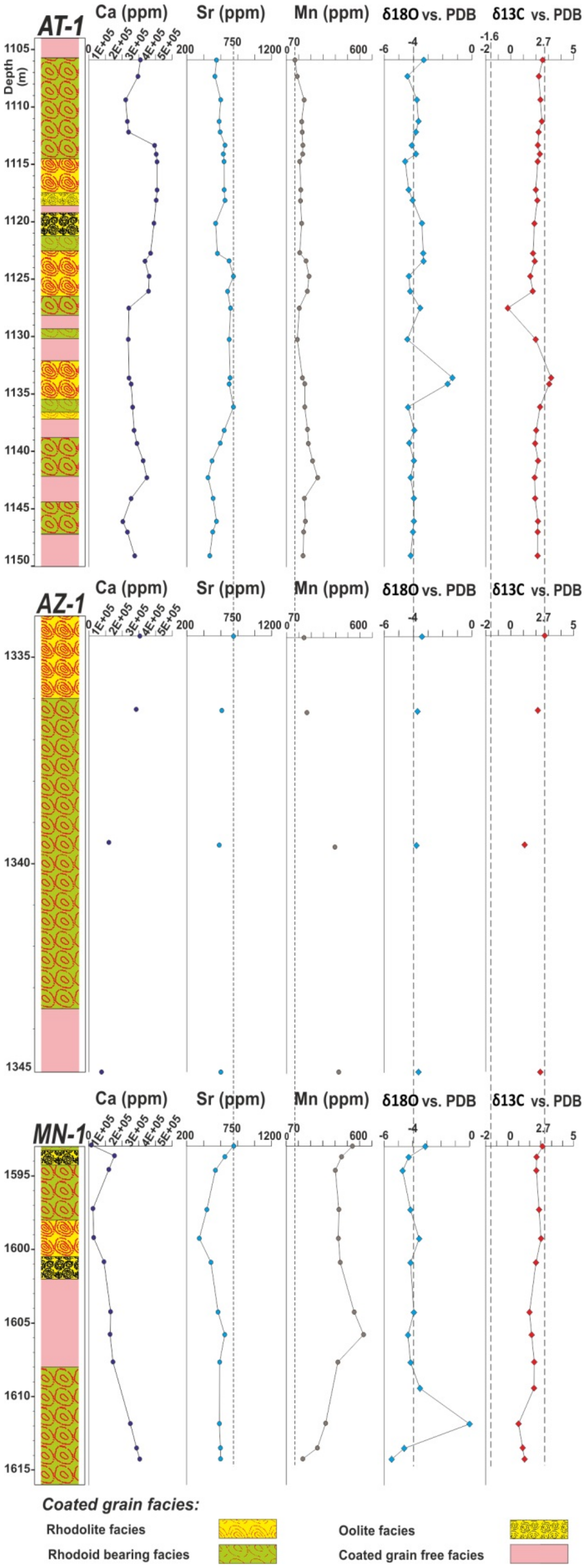


Figure 6. Elemental Ca, Sr and Mn, and oxygen and carbon stable isotope ratios of the coated grain bearing part of the Ilam Formation at the studied fields. Maximum value of Sr is 750 ppm (dashed line). Dashed line on the Mn log is considered as diagenetic alteration cut-off. Samples with >70 ppm values are diagenetically altered (Al-Aasm & Veizer, 1986). Generally, values of oxygen and carbon stable isotopes are consistent with the Cretaceous marine limestone signature ($\delta^{18}O$: -4 to 1.1‰; $\delta^{13}C$: -1.6 to 2.7‰; Veizer *et al*., 1999).

## Primary mineralogy

*Petrographic evidence*

Many ooids show radial-fibrous internal fabrics that are considered to be primary and originally calcite (LMC; Fig. 4d; Shearman *et al*., 1970; Bathurst, 1975; Sandberg, 1975). There is no (diagenetic) evidence of unstable original mineralogy such as oo-mold, replaced ooids etc. (e.g. Enayati-Bidgoli & Rahimpour-Bonab, 2016). Also, concomitant bivalve and gastropod shells are replaced by calcite cement through aragonite stabilization and/or dissolution and replacement which indicate more resistant carbonate mineralogy of ooids (Figs. 7a and 7b; Wilkinson *et al*., 1984; Haggerty & Silva, 1986).

The original internal fabric of rhodoids (which mainly originated by red algal thalli; Peryt, 1983; Flügel, 2010) is well preserved (Figs. 5a–5d and 7c). Moreover, some rhodoids are partially to completely replaced by yellowish rhombic dolomite crystals (Figs. 7d to 7f) as fabric selective dolomitization (Fig. 7d). Most likely, HMC has been the primary mineralogy of rhodoids (related to red algae; Schlanger, 1957; Milliman, 1974; Burgess & Anderson, 1983) that locally provided Mg ions for dolomitization and selectively dolomitized rhodoids (Figs. 7a to 7e). Other evidence is the corrosive effect of dolomitizating fluids on rhodoids (Fig. 7f), and their higher resistance against the meteoric fluids in comparison with the mineralogically stabilized aragonitic allochems such as bivalves in a certain sample (Fig. 7g).

*Geochemical evidence*

The average Sr content of the samples (both with and without coated grains) with 571 ppm concentration (Fig. 6) is higher than unaltered Cretaceous marine carbonates (about 320 ppm; Veizer, 1977). In modern carbonate sediments, Sr ranges between 3000 and 10000 ppm Sr. Aragonitic ooids and lime muds precipitated from seawater have 8000–10000 ppm that is inconsistent with the Sr content of seawater (Kinsman, 1969). The Sr content of aragonitic bioclasts is also several thousand ppm (e.g. Land and Hoops, 1973).

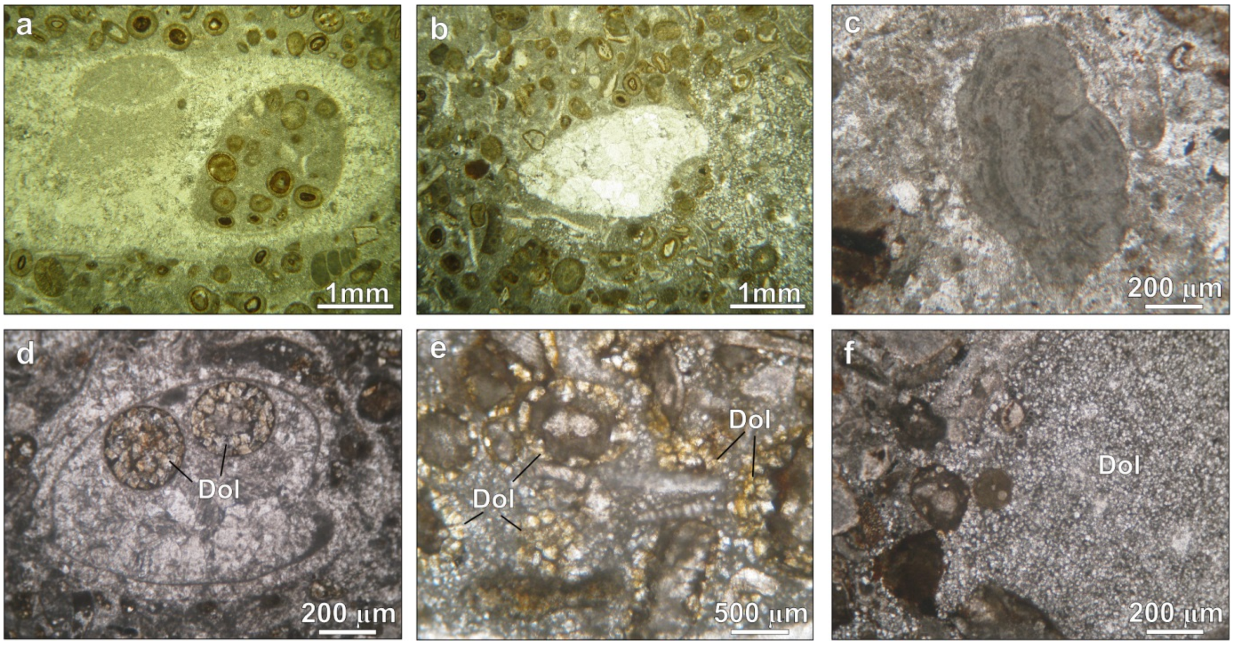


Figure 7. Petrographic evidence (depositional and diagenetic) that is related to the primary mineralogy of the coated grains. a–b Stabilized (primarily aragonitic) gastropod and bivalve in a same thin section with unaltered LMC ooids; c Unaltered internal structure of a single rhodoid; d–e Selective growth of rhombic dolomite crystals (Dol) in relation with rhodoids; f Corrosive effect of secondary dolomitizing fluids on rhodoids as a result of higher susceptibility of HMC mineralogy.

Calcitic skeletal grains and HMC cements have much lower strontium contents (around 1000 ppm; Tucker, 1985). Many ancient limestones have Sr content of only several hundred ppm (e.g. Kinsman, 1969: Veizer & Demovic 1974), which can be due to (Tucker, 1985): (a) neomorphic processes such as calcitization of aragonite (Figs. 7h to 7i) and calcite recrystallization (Figs. 4e, 5c and 7a), (b) late sparry calcite cements precipitated from low Sr meteoric (Figs. 4c, 4d and 5g, 5h and 7g to 7i) and meteoric–marine pore waters (Figs. 5a, 5b, 5d to 5g and 5i), (c) the mid-Paleozoic and later Mesozoic carbonate rocks were deposited as calcite with little aragonite and low initial Sr content.

However, rather than neomorphic processes and meteoric/marine sparry calcite cementation (as above), relatively higher Sr concentrations in the analyzed samples compared to unaltered Cretaceous marine carbonates (Veizer, 1977) can be due to argillaceous content (Fig. 3) and influx of terrigeneous material (Navidtalab *et al*., 2016). Through the decay process, $^{87}$Rb can transform to $^{87}$Sr with passing time. $^{87}$Rb is abundant in terrigenous materials such as clay and siliciclastic minerals, incorporating in carbonates via infiltrating meteoric waters. This might happen in the Ilam carbonates due to its higher terrigenous content (Fig. 3) and mineral stabilization via percolating meteoric waters (Navidtalab *et al*., 2016).

Carbon and Oxygen stable isotopes cross plot of the studied intervals are compared with literatures (Fig. 8a). Approximately, all analyzed samples fall in the presented domains for Cretaceous marine limestone (Fig. 8a). There is no differentiation between the analyzed samples based on their allochemical components (Fig. 8a). Regarding the Sr and stable isotopes values and petrographic evidence (low volume of mineralogically stabilized aragonitic bioclasts), calcite (LMC and HMC) could be considered as the original mineralogy of the studied intervals (Figs. 4 to 7).

Mn content shows that approximately all samples from the studied wells (especially, MN-1 and to some extent AZ-1 samples) experienced diagenetic alteration in a relatively semi-closed system (Figs. 6 and 8b and 8c). In general, Mn contents >70 ppm are considered to represent diagenetic imprints (Fig. 6; e.g. Al-Aasm & Veizer, 1986). Mn—Sr/Ca diagram shows that most of the Ilam carbonates are diagenetically altered in a partly closed system (Fig. 8b), some samples such as MN-1 are affected by an open diagenetic system (Fig. 8b). $\delta^{18}$O—Mn cross-plot denotes the imprint of diagenetic alteration in the Ilam carbonates that occurred in a relatively closed system, but samples from well MN-1 are highly altered in an open diagenetic system (Fig. 8c).

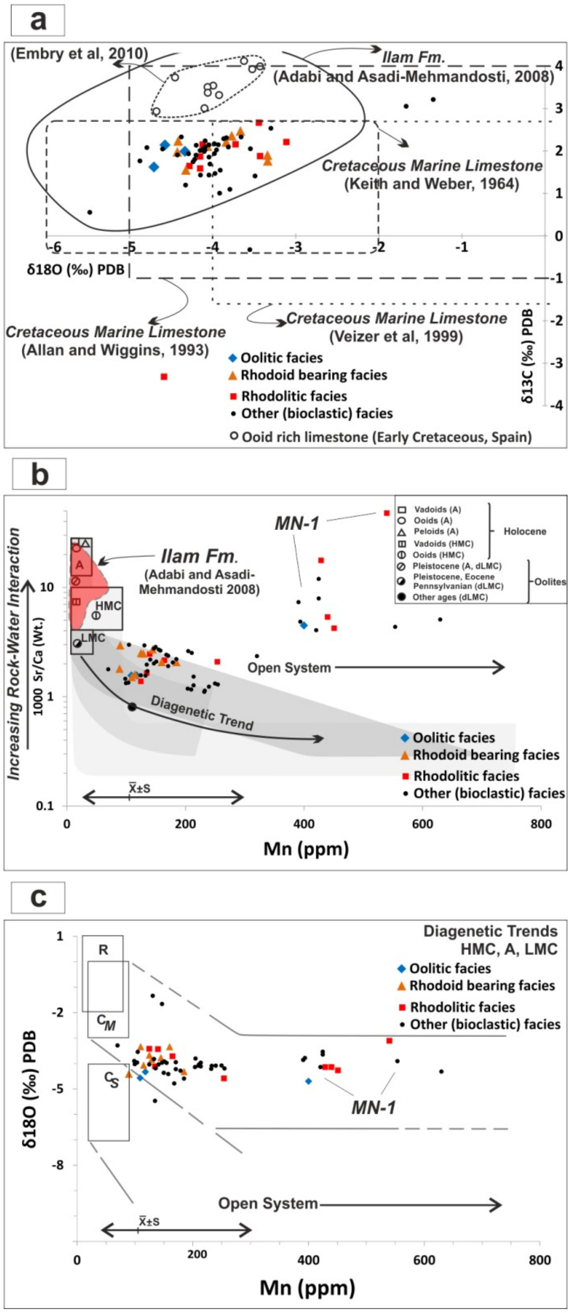

Figure 8. a: Oxygen and carbon stable isotope values of the Ilam Formation in the studied wells are compared with domains of the Cretaceous marine limestone (Keith & Weber, 1964; Allan & Wiggins, 1993; Veizer *et al*., 1999), Early Cretaceous ooid-rich limestone (Embry *et al*., 2010) and Ilam Formation in Tang-E Rashid area (Adabi & Asadi-Mehmandosti, 2008). Approximately, all analyzed samples fall in the presented domains for the Cretaceous marine limestone. There is not any differentiation between the analyzed samples based on their allochemical component. b: and Sr/Ca–Mn cross-plot variations in the Ilam carbonates.. MN-1 samples are affected by an open diagenetic system (Brand & Veizer, 1980). c: δ $^{18}$O vs. Mn cross-plot (Brand & Veizer, 1981) with diagenetic stabilization trends for the presumed originally HMC, aragonite, and LMC carbonate components shows that Ilam carbonates are diagenetically altered in a relatively closed system ($\overline{x}\pm s$; Brand & Veizer, 1980) but samples from the MN-1 well are highly altered in an open diagenetic system. The R (Recent) and $C_M$ (Mississippian) and $C_S$ (Silurian) fields are the postulated ranges for carbonates (HMC, A, and LMC) in equilibrium with contemporaneous sea water (Lowenstam, 1961; Perry, 1967; Fritz, 1971; Milliman, 1974; Veizer & Hoefs, 1976).

This open system led to leaching of Ca and probably increasing of radiogenic Sr, driving the samples toward upper right corner rather than lower right. Due to whole rock sampling, geochemical data provides only a rough view.

## Discussion

The Ilam Formation deposited during the transition from a very warm (middle Cretaceous) to a relatively cool (late Cretaceous) climates (Douglas & Savin, 1973, 1975; Arthur *et al*., 1985; Barrera *et al*., 1987; Barrera *et al*., 1997; Spicer & Corfield, 1992; D'Hondt & Lindinger, 1994; Huber *et al*., 1995; D'Hondt & Arthur, 1996; Li & Keller, 1998a, b). Regarding the oscillatory trend in mineralogy of carbonate allochems through the Phanerozoic (Figs. 9a and 9b; Sandberg, 1975, 1983; Mackenzie & Pigott, 1981; Wilkinson *et al*., 1982) there is a global increase of calcitic ooids until Cretaceous time (Fig. 9c; Mackenzie & Agegian, 1989). Parameters such as intense seafloor spreading (Figs. 1a and 1b) and higher $CO_2$ levels in the ocean-atmosphere system (Mackenzie & Piggott, 1981; Gaffin, 1987; Berner, 1990; Cerling, 1991), global highstand (Fig. 9c; Pitman, 1978; Schlanger *et al*., 1981; Hallam, 1984; Haq *et al*., 1987) and consequently low saturation of seawater with respect to carbonate minerals as a result of decreased Mg/Ca ratio in seawater (Jenkyns & Strasser, 1995), and mixing of sea water with ground water (Plummer,, 1975; Laabidi & Bouhlila, 2016) have been in favor of calcite precipitation (Chatalov, 2005).

Globally, the Late Cretaceous is known as one of the few periods with low occurrence of ooids. At this time, all deposited ooids have primary radial fabric, and calcite mineralogy (Figs. 9c and 9d). As shown, in the Ilam carbonates, petrographical and geochemical evidence are consonant with the global characteristics of the Late Cretaceous ooids.

Seemingly, in the Ilam platform, there has been very low opportunity for a good assemblage of all required parameters such as shallow and agitated water (3–5m), supersaturation with $CaCO_3$, warming, degassing, and flowing over low-relief hard substrate (Dravis, 1979; Simone, 1981) to produce ooids.

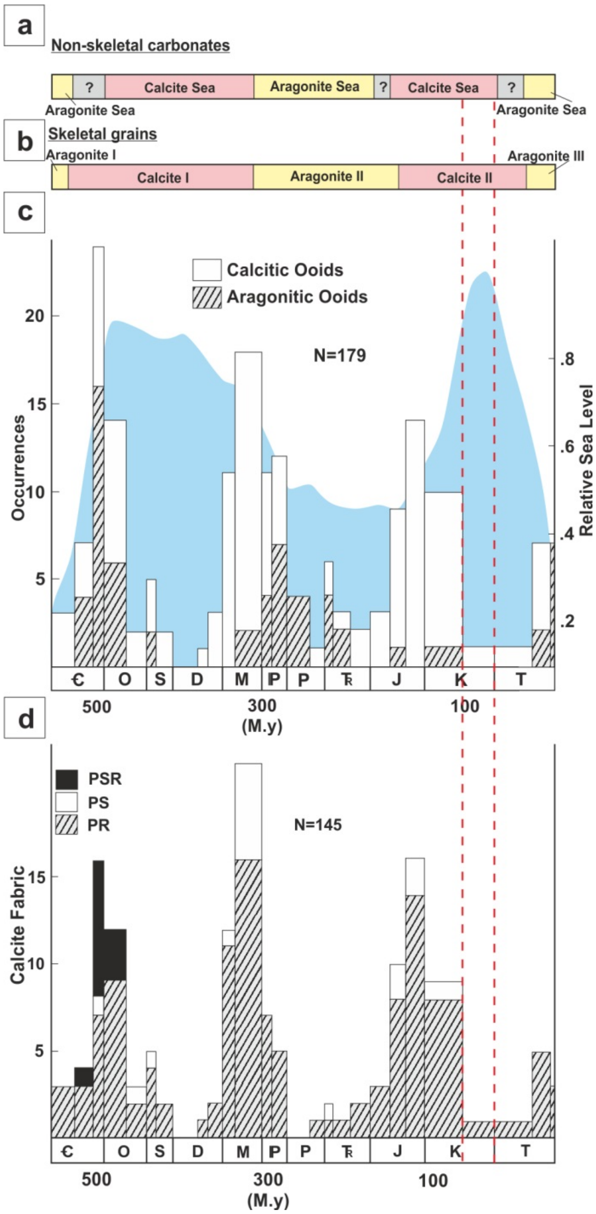


Figure 9 a. The Sandberg model (Sandberg, 1983, 1985) for non-skeletal carbonates (ancient ooids and cements) indicates timespans dominated by aragonite and HMC, and timespans dominated by calcite through the Phanerozoic such as the Late Cretaceous. b: The Stanley-Hardie model (Stanley & Hardie 1998) describes secular oscillations in the carbonate mineralogy of skeletal carbonates (hypercalcifying reef-building and sediment-producing organisms). c: Temporal distribution of originally calcite and aragonite ooid cortices through the Phanerozoic (Wilkinson *et al*., 1985). Global sea level (blue background) is from Vail *et al*. (1977). As shown by global pattern, ooids of the Ilam Formation are expected to have primary calcite mineralogy, created during a global highstand. d: Distribution of calcite fabrics which shows primary cortical calcite for the studied time interval. PR: primary radial; PS: primary spalled radial; FSR: primary sparry radial. Radial fabrics predominate in calcitic ooids (Wilkinson *et al*., 1985).

Creation of a subduction zone due to the initiation of Neo-Tethys closure in the Zagros domain (Sepehr & Cosgrove, 2004; Navidtalab *et al*., 2016) is compatible with the Mackenzie & Pigott scheme (1981) about the calcite seas (higher $PCO_2$ and lower Mg/Ca).

These fine ooids may be resulted due to high nuclei supply, lower growth rate, lower agitation level and mobilization, abrasion (Bathurst, 1975; Medwedeff & Wilkinson, 1983; Swett & Knoll, 1989; Sumner & Grotzinger, 1993), and lower saturation of carbonate in sea water.

After the mid-Turonian exposure in the studied area (Dezful Embayment), the former Sarvak platform was drowned and the relatively deep water facies were deposited on the newly established Ilam platform. Then, toward the upper Ilam, deep facies are replaced by relatively shallower rhodolitic/oolitic facies (Fig. 3). These thin oolitic intervals with diverse bioclasts such as gastropod and echinoderm, bivalve, bryozoa, and rudist fragments indicate high-energy environment. It developed on the shallow ramp (Mehrabi *et al*, 2014) under strong action of tidal and wave currents during the formation of the ramp carbonate platform favorable for reworking of sedimentary grains on the sea floor and formation of high-energy ooids especially on proximal mid ramp setting (Simone, 1981; Flügel, 1982, 2004; Tucker & Wright, 1990; Gerdes *et al*., 1994; Mei *et al*., 1997; Siewers, 2003; Brehm *et al*., 2003, 2006; Reeder & Rankey, 2008). However, the only reported oolitic interval at top the Tanuma Formation (the only reported ooid bearing interval from the stratigraphic equivalents of the Ilam Formation of the Arabian Plate) in the southern Iraq (Owen & Nasr, 1958; Bellen *et al*., 1959) contains ooids which have been dissolved partially and filled by calcite cement. The large size of the ooids, their thin cortical lamellas and the micritic groundmass are interpreted as low energy depositional conditions (Sadooni, 2004).

In comparison with oolitic intervals, rhodolitic and rhodoid bearing units form higher portion of the upper part of the Ilam that developed during highstand systems tract (Fig. 3). The detected rhodoids in the Ilam carbonates are very finer than centimeter-sized typical rhodoids (Flügel, 2010). Generally, light is the most important control on the growth of rhodoids (red algae). Ancient rhodalgal-type grain associations are often indicative of platforms formed in temperate seas or in subtropical to tropic areas (Flügel, 2010). According to these illustrations, and also defined characteristics of the detected rhodoids and their association with echinoderm fragments (mid ramp setting; Flügel, 2004), the upper part of the Ilam represents the mid ramp setting with relatively low agitation and periodical turbulences which led to reworked rhodoids (Fig. 4l). But, in the Gachsaran and Rag-e Sefid fields, due to deeper depositional setting (mainly outer ramp facies), there is not any coated grain which are mostly indicative of mid-ramp and inner ramp settings (Fig. 3).

Generally, the grain association in the (upper) Ilam and their mineralogy–including LMC ooids and bioclasts (bivalve), HMC rhodoids and bioclasts (echinoderm fragments), and some aragonitic bioclasts (now are calcite)–represent subtropical-temperate climatic setting (likely rhodalgal; Flügel, 2010; Simone *et al*., 2012). These mineralogy and grain associations are related to the Late Cretaceous cooling and recovery of the carbonate factory after the early–middle Turonian hyper-greenhouse condition/crisis (Simone, *et al*. 2012). In fact, regarding the small drift of the Arabian Plate (10-15º N latitudes) throughout the Cretaceous, the difference between allochemical content of the Sarvak (middle Cretaceous) and Ilam (Coniacian–Maastrichtian) could be ascribed to the changes in paleoclimate from warm/very warm during the mid-Cretaceous to cooler conditions in the Coniacian–Maastrichtian (Huber *et al*., 2002; Fluteau *et al*., 2007; Keller *et al*., 2008).

In the mid-Cretaceous Sarvak Formation and its equivalents, rudists are the main biologic colonies (e.g. Mishrif Formation; Alsharhan & Nairn, 2003). In the Ilam, the abundance of rudist communities is lower than the Sarvak and there is some evidence for other colonized communities such as bryozoans. In the Sravak successions, echinoderm fragments are dominant. They are accompanied by rhodoids in the Ilam Formation. The existence of rhodoids is remarkable. They started to dominate from Late Mesozoic to Cenozoic (Flügel, 2010).

## Conclusions

The upper part of the Ilam Formation in three of the five studied oilfields of the Dezful Embayment contains several morphologically different coated grains including ooids and rhodoids.

The recognized rhodoids in the Ilam Formation are sub-divided into five types including: superficial, concentric, compound, loose, and reworked.

Three types of ooids including superficial, concentric-radial, and compound can be detected in the Ilam Formation.

Compared to unaltered Cretaceous marine carbonates, relatively higher Sr concentrations of the analyzed samples could be ascribed to argillaceous content from shale intervals. However, these concentrations are similar to calcitic skeletal grains and HMC cements that bear a testimony to the original mineralogy of calcite for the analyzed samples.

Petrographical and geochemical evidences showed that the ooids and rhodoids of the Ilam Formation have been originally LMC and HMC, respectively.

The existence of calcitic ooids (late Cretaceous) was consistent with the oscillatory trend in mineralogy of ooids through the Phanerozoic.

The scarcity of oolitic intervals in the studied subsurface sections indicated that necessary parameters for ooids generation have been temporary and local.

The presence of LMC ooids and HMC rhodoids were compatible with the Late Cretaceous cooling phase which led to rhodalgal like grain assemblage.

## Acknowledgements

The University of Tehran provided facilities for this research for which the authors are grateful. NISOC is thanked for support and data preparation. H Mohseni and an anonymous reviewer are thanked for their review and comments that improved this paper.

## References

Adabi, MH., Asadi-Mehmandosti, E,. 2008. Microfacies and geochemistry of the Ilam Formation in the Tang-E-Rashid area, Izeh, SW Iran. Journal of Asian Earth Sciences, 33: 267–277.

Aghanabati, A., 2004. Geology of Iran. Geological survey of Iran, Tehran [in Persian].

Al-Aasm, IS., Veizer, J., 1986. Chemical stabilization of aragonite and low-Mg calcite: An example of brachiopods. Journal of Sedimentary Petrology, 52: 1101–1109.

Alavi, M., 2004. Regional stratigraphy of the Zagros fold-thrust belt of Iran and its proforeland evolution. American Journal of Science, 304: 1–20 .

Alavi, M., 2007. Structures of the Zagros fold-thrust belt in Iran. American Journal of Science, 307: 1064–1095.

Allan, JR., Wiggins, WD., 1993. Dolomite reservoirs – geochemical techniques for evaluating origin and distribution. American Association of Petroleum Geologists, Short Course Note Series 36, Tulsa.

Alsharhan, AS., 1989. Petroleum geology of the United Arab Emirates. Journal of Petroleum Geology, 12: 253–288.

Alsharhan, AS., Kendall, CGStC., 1995. Facies variation, depositional setting and hydrocarbon potential of the Upper Cretaceous rocks in the U.A.E. Cretaceous Research, 16: 435–449.

Alsharhan, AS., Nairn, AEM., 1993. Carbonate platform models of Arabian Cretaceous reservoirs. In: Simo JAT, Scott RW, Masse JP., eds. Cretaceous carbonate platforms. American Association of Petroleum Geologists Memoir, 56: 173–184.

Alsharhan, AS., Nairn, AEM., 2003. Sedimentary basins and petroleum geology of the Middle East. Elsevier, Amsterdam.

Aqrawi, AAM., Thehni, GA., Sherwani, GH., Kareem, BMA., 1998. Mid-Cretaceous rudist bearing carbonates of the Mishrif formation: an important reservoir sequence in the Mesopotamian basin, Iraq. Journal of Petroleum Geology, 21: 57–82

Arthur, MA., Dean, WE., Schlanger, SO., 1985. Variations in the global carbon cycle during the Cretaceous related to climate, volcanism, and changes in atmospheric CO2. In: Sunquist, ET., Broecker, WS. (eds). The Carbon Cycle and Atmospheric CO2: Natural Variations Archean to Present. American Geophysical Union, 32: 504–529.

Barrera, E., Huber, BT., Savin, SM., Webb, PN., 1987. Antarctic marine temperatures: late Campanian through Early Paleocene. Paleoceanography, 2: 21–47.

Barrera, E., Savin, SM., Thomas, E., Jones, CE., 1997. Evidence for thermohaline-circulation reversals controlled by sea-level change in the latest Cretaceous. Geology, 25: 715–718.

Bathurst, RGC., 1971. Carbonate sediments and their diagenesis. Developments in Sedimentology 12, Elsevier, Amsterdam.

Bellen, RC., van Dunnington, HV., Wetzel, R., Morton, DM., 1959. Iraq: Lexique Strat. International Centre National Rechearche Scientifique, Paris, III, Asie, Fasc, 10a: 333 p.

Berner, RA., 1990. Atmospheric carbon dioxide level over Phanerozoic time. Science, 249: 1382–1386.

Beydoun, ZR., 1991. Arabian plate hydrocarbon geology and potential: a plate tectonic approach. American Association of Petroleum Geologists, Studies in Geology, 33.

Beydoun, ZR., Hughes Clarke, MW., Stoneley, R., 1992. Petroleum in the Zagros Basin: a late Tertiary foreland basin overprinted onto the outer edge of a vast hydrocarbon-rich Paleozoic-Mesozoic passive margin shelf. In: Macqeen, R., Leckie, DA. (eds). Foreland Basins and Fold Belts. American Association of Petroleum Geologists Memoir 55: 309–339.

Brand, U., Veizer, J., 1980. Chemical diagenesis of a multicomponent carbonate system 1: trace elements. Journal of Sedimentary Petrology, 50: 1219–1236.

Brand, U., Veizer, J., 1981. Chemical diagenesis of a multicomponent carbonate system 2: stable isotopes. Journal of Sedimentary Research, 51: 987–997.

Burgess, CJ., Anderson, JM., 1983. Rhodoids in temperate carbonates from the Cenozoic of New Zealand. In: Peryt, TM. (ed). Coated Grains. Springer-Verlag, Berlin Heidelberg, pp 243–258.

Buxton, MWN., Pedley, M., 1989. Short paper: a standardized model for Tethyan Tertiary carbonates ramps. Geological Society of London, 146: 746–748

Carozzi, AV., 1957. Contribution de l'etude des proprietes geomètriques des oolithes l'exemple du Grand Lac Sale, Utah, USA. Bulletin de l'Institut National Genevois, 58: 1–52.

Cater, JML., Gillcrist, JR., 1994. Karstic reservoirs of the Mid-Cretaceous Mardin Group, SE Turkey: Tectonic and eustatic controls on their genesis, distribution and preservation. Journal of Petroleum Geology, 17: 253–278.

Casini, G., et al., 2011. Sub-seismic fractures in foreland fold and thrust belts: insight from the Lurestan Province, Zagros Mountains, Iran. Petroleum Geoscience, 17: 263–282.

Cerling, TE., 1991. Carbon dioxide in the atmosphere: evidence from Cenozoic and Mesozoic paleosols. American Journal of Science, 291: 377–400.

Chatalov, AG., 2005. Aragonitic-calcitic ooids from Lower to Middle Triassic peritidal sediments in the western Balkanides, Bulgaria. Neues Jahrbuch fuer Geologie und Paleontologie, Abhandlungen 237, 1: 87–110.

Christian, L., 1997. Cretaceous Subsurface Geology of the Middle East Region. GeoArabia 2: 3.

D'Hondt, S., Lindinger , M., 1994. A stable isotopic record of the Maastrichtian ocean–climate system: South Atlantic DSDP Site 528. Paleogeography, Paleoclimatology, Paleoecology, 112: 363–378.

D'Hondt, S., Arthur, MA., 1996. Late Cretaceous oceans and the cool tropic paradox. Science, 271: 1838–1841.

Davies, PJ., Bubela, B., Ferguson, F., 1978. The formation of ooids. Sedimentology, 25: 703–730.

Douglas, RG., Savin, SM., 1973. Oxygen and carbon isotope analysis of Cretaceous and Tertiary foraminifera from the central North Pacific. Initial Reports of Deep Sea Drilling Project, 17:591–605.

Dravis, J., 1979. Rapid and widespread generation of recent oolitic hardgrounds on a high energy Bahamian platform,

Eleuthera Bank, Bahamas. Journal of Sedimentary Petrology, 49: 195–208.
Duguid, SMA., Kyser, TK., James, NP., Rankey, EC., 2010. Microbes and ooids. Journal of Sedimentary Research, 80: 236–251.
Embry, J-C., Vennin, E., van Buchem, FSP., Schroeder, R., Pierre, C., Aurell, M., 2010. Sequence stratigraphy and carbon isotope stratigraphy of an Aptian mixed carbonate-siliciclastic platform to basin transition., Galve sub-basin, NE Spain.. In: van Buchem, FSP., Gerdes, KD., Esteban, M. (eds). Mesozoic and Cenozoic Carbonate Systems of the Mediterranean and the Middle East: Stratigraphic and Diagenetic Reference Models. Geological Society of London Special Publications, 329: 112–143.
Enayati- Bidgoli, A.H., Rahimpour-Bonab, H., 2016. A geological based reservoir zonation scheme in a sequence stratigraphic framework: A case study from the Permo-Triassic gas reservoirs, Offshore Iran. Marine and Petroleum Geology, 73: 36-58.
Flügel, E., 1982. Microfacies analysis of limestones. Springer, Berlin.
Flügel, E., 2004. Microfacies of carbonate rocks. Springer, Berlin Heidelberg New York.
Flügel, E., 2010. Microfacies of carbonate rocks: analysis, interpretation and application, 2nd edn. Springer, Berlin Heidelberg New York.
Fluteau, F., Ramstein, G., Besse, J., Guiraud, R., Masse, J-P., 2007. Impacts of paleogeography and sea level changes on Mid-Cretaceous climate. Paleogeography, Paleoclimatology, Paleoecology, 247: 357–381.
Folk, RL., 1993. SEM imaging of bacteria and nannobacteria in carbonate sediments and rocks. Journal of Sedimentary Petrology, 63: 990–999.
Fritz, P., 1971. Geochemical characteristics of dolomites and the 18O content of Middle Devonian oceans. Earth and Planetary Science Letters, 11: 277–282.
Ghabeishavi, A., Vaziri-Moghaddam, H., Taheri, A., 2009. Facies distribution and sequence stratigraphy of the Coniacian–Santonian succession of the Bangestan Paleo-high in the Bangestan Anticline, SW Iran. Facies, 55: 243–257
Gaffin, S., 1987. Ridge volume dependence on seafloor generation rate and inversion using long term sea level change. American Journal of Science, 287: 596–611.
Glennie, KW., Boeuf, MGA., Hughes-Clarke, MW., Moody-Stuart, M., Pilaar, WFH., Reinhardt, BM., 1974. Geology of the Oman Mountain. Royal Geological and Mining Society of the Netherlands, 31: 423 p.
Haggerty, JA., Premoli-Silva, I., 1986. Ooids and shallow-water debris in Aptian-Albian sediments from the East Mariana Basin, Deep Sea Drilling Project Site 585: implications for the environment of formation of the ooids. In: Moberly, R., Schlanger, SO., et al. (eds). Initial reports of the DSDP covering Leg 89 of the cruises of the Drilling Vessel Glomar Challenger, Yokohama, Japan, to Noumea, New Caledonia: Washington., United States Government Printing Office, pp 399–412.
Hallam, A., 1984. Pre-Quaternary sea level changes. Annual Review of Earth and Planetary Sciences, 12: 205–243.
Haq, BH., Hardenbol, J., Vail, PR., 1987. Chronology of fluctuating sea levels since the Triassic. Science, 235: 1156–1167.
Harris, PM., 1979. Facies anatomy and diagenesis of a Bahamian ooid shoal. Sedimenta 7, Comparative Sedimentology Laboratory, University of Miami, Florida.
Hart, BB‘t., 1970a. Upper Cretaceous paleogeography, structural history and prospect of Khuzestan Province, Iran. Iranian Oil Operating Companies, report No. 1172 (unpublished).
Hart, BB‘t., 1970b. Tectonic framework and paleogeography of the agreement area. Iranian Oil Operating Companies, report No. 1179 (unpublished).
Heller, PL., Komar, PD., Pevear, DR., 1980. Transport processes in ooid genesis. Journal of Sedimentary Petrology, 50: 943–952.
Heydari, E., 2008. Tectonic versus eustatic control on supersequences of the Zagros Mountains of Iran. Tectonophysics, 451: 56–70
Hillgärtner, H., Dupraz, C., Hug, W., 2001. Microbially induced cementation of carbonate sands: are micritic meniscus cements good indicators of vadose diagenesis? Sedimentology, 48:117–131. doi:10.1046/j.1365-3091.2001.00356.x
Hollis, C., 2011. Diagenetic controls on reservoir properties of carbonate successions within the Albian–Turonian of the Arabian Plate. Petroleum Geoscience, 17: 223–241
Huber, BT., Hodell, DA., Hamilton, CP., 1995. Middle-Late Cretaceous climate of the southern high latitudes: stable isotopic evidence for minimal equator-to-pole thermal gradients. Geological Society of America Bulletin, 107: 1164–1191.
Huber, BT., Norris, RD., Macleod, KG., 2002. Deep-sea paleotemperature record of extreme warmth during the Cretaceous. Geology, 30: 123–126
James, GA., Wynd, JG., 1965. Stratigraphic nomenclature of Iranian oil consortium, agreement area. American Association of Petroleum Geologists Bulletin, 49: 2182–2245
Jenkyns, HC., Strasser, A., 1995. Lower Cretaceous oolites from the Mid-Pacific Mountains., Resolution Guyot, Site

866. In: Winterer, EL., Sager, WW., Firth, JV., Sinton, JM. (eds). Proc. ODP, Sci. Results, 143: College Station, TX., Ocean Drilling Program, 111–118 .
Keith, ML., Weber, JN., 1964. Carbon and oxygen isotopic composition of selected limestones and fossils. Geochimica et Cosmochimica Acta, 28: 1787–1816.
Keller, G., Adatte, T., Berner, Z., Chellai, EH., Stueben, D., 2008. Oceanic events and biotic effects of the Cenomanian–Turonian Anoxic event, Tarfaya basin, Morocco. Cretaceous Research, 29: 976–994.
Kent, PE., Slinger, ECP., Thomas, AN., 1951. Stratigraphical exploration surveys in southwest Persia. Proceedings of the 3rd World Petroleum Congress, The Hague, Section 1: 141–161.
Khalili, M., 1974. The biostratigraphic synthesis of the Bangestan Group in southwest Iran. Oil service company of Iran report 1219 (unpublished.(
Kinsman, DJJ., 1969. Interpretation of Sr2+ concentrations in carbonate minerals and rocks. Journal of Sedimentary Petrology, 39: 486–508
Koop, W., Stoneley, R., 1982. Subsidence history of the Middle East Zagros basin, Permian to Recent. Philosophical Transactions of the Royal Society, 305: 149–168
Laabidi, E., Bouhlila, R., 2016. Impact of mixing induced calcite precipitation on the flow and transport. Carbonates and Evaporites, 1–13 .
Land, LS., Hoops, GK., 1973. Sodium in carbonate sediments and rocks: possible index to the salinity of diagenetic solutions. Journal of Sedimentary Petrology, 43: 614–617.
Li, L., Keller, G., 1998a. Maastrichtian climate, productivity and faunal turnovers in planktic foraminifera in south Atlantic DSDP Site 525A and 21. Marine Micropaleontology, 33: 55– 86.
Li, L., Keller, G., 1998b. Abrupt deep sea warming at the end of the Cretaceous. Geology, 26 :995–998.
Lowenstam, HA., 1961. Mineralogy, O18/O16 ratios, and strontium and magnesium contents or Recent and fossil brachiopods and their bearing on the history of tile oceans. Journal of Geology, 69: 241–260.
Mackenzie, FT., Pigott, JD., 1981. Tectonic controls of Phanerozoic sedimentary rock cycling. Geological Society of London, 138: 183–196.
Mackenzie, FT., Agegian, CR., 1989. Biomineralization and tentative links to plate tectonics, In: Crick RE., ed. Origin, evolution and modern aspects of biomineralization in plants and animals. Plenum Press, New York, pp 11–27.
Medwedeff, DA., Wilkinson, BH., 1983. Cortical fabric in calcite and aragonite ooids. In: Peryt TM., ed. Coated Grains. New York., Springer-Verlag., pp 109–115.
Mehrabi, H., Rahimpour-Bonab, H., Enayati-Bidgoli, AH., Navidtalab, A., 2014. Depositional environment and sequence stratigraphy of the Upper Cretaceous Ilam Formation in central and southern parts of the Dezful Embayment, SW Iran. Carbonate Evaporate, 29: 263–278. doi:10.1007/s13146-013-0168-z
Mehrabi, H., Rahimpour-Bonab, H., 2014. Paleoclimate and tectonic controls on the depositional and diagenetic history of the Cenomanian-Early Turonian carbonate reservoirs, Dezful Embayment, SW Iran. Facies, 60: 147–167 .
Mei, MX., Ma, YS., Zhou, PK., Su, DC., Luo, GW., 1997. Introduction to Carbonate Sedimentology. Seismological Press, Beijing, in Chinese.
Mei, MX., Gao, J., 2012. Giant Induan oolite: A case study from the Lower Triassic Daye Formation in the western Hubei Province, South China. Geoscience Frontiers, 3(6): 843–851.
Middleton, GV., 1976. Hydraulic interpretation of sand size distributions. Journal of Geology, 84: 405–426.
Miller, MC., McCave, IN., Komar, PD., 1977. Threshold of sediment motion under unidirectional currents. Sedimentology, 24: 507–527.
Milliman, JD., 1974. Recent Sedimentary Carbonates. Part 1 Marine Carbonates. Springer, Berlin Heidelberg New York.
Motiei, H., 1993. Geology of Iran, stratigraphy of Zagros. Treatise on the Geology of Iran, Geological survey of Iran, Tehran [in Persian.[
Murris, RJ., 1980. Middle East: stratigraphic evolution and oil habitat. American Association of Petroleum Geologists Bulletin, 64: 597–618
Navidtalab, A., Rahimpour-Bonab, H., Huck, S., Heimhofer, U., 2016. Elemental geochemistry and strontium-isotope stratigraphy of Cenomanian to Santonian neritic carbonates in the Zagros Basin, Iran. Sedimentary Geology, 346: 35-48.
Navidtalab, A., Sarfi, M., Enayati-Bidgoli, A., Yazdi-Moghadam, M., 2019. Syn-depositional continental rifting of the southeastern Neo-Tethys margin during the Albian–Cenomanian: evidence from stratigraphic correlation. International Geology Review. doi: 10.1080/00206814.2019.1667882
Owen, RMS., Nasr, SN., 1958. The stratigraphy of the Kuwait-Basrah area. In: Weeks GL., ed. Habitat of Oil a Symposium. American Association of Petroleum Geologists, Tulsa
Pedley, M., 1998. A review of sediment distributions and processes in Oligo-Miocene ramps of southern Italy and Malta., Mediterranean divide.. In: Wright VP, Burchette TP., eds. Carbonate ramps. Geological Society of London Special Publication, pp 163–179.

Perry, ECJR., 1967. The oxygen isotope chemistry of ancient cherts. Earth and Planetary Science Letters, 3: 62–66.
Peryt, TM., 1983. Classification of coated grains. In: Peryt, TM. (ed). Coated Grains. Springer-Verlag, Berlin, pp 142–153.
Pitman, WC., 1978. Relationship between eustacy and stratigraphic sequences of passive margins. Geological Society of America Bulletin, 89: 1389–1403.
Plummer, LN., 1975. Mixing of sea water with calcium carbonate ground water. Geological Society of America Memoir, 142: 219–236. doi:10.1130/MEM142p219
Rahimpour-Bonab, H., Mehrabi, H., Enayati-Bidgoli, AH., Omidvar, M., 2012a. Coupled imprints of tropical climate and recurring emersions on reservoir evolution of a Mid-Cretaceous carbonate ramp, Zagros Basin, SW Iran. Cretaceous Research, 37: 15–34
Rahimpour-Bonab, H., Mehrabi, H., Navidtalab, A., Izadi-Mazidi, E., 2012b. Flow unit distribution and reservoir modeling in Cretaceous carbonates of the Sarvak Formation, Abteymour oilfield, Dezful Embayment, SW Iran. Journal of Petroleum Geology, 35(3): 213–236
Rahimpour-Bonab, H., Mehrabi, H., Navidtalab, A., Omidvar, M., Enayati-Bidgoli, AH., Sonei, R., Sajjadi, F., Amiri-Bakhtiar, H., Arzani, N., Izadi-Mazidi, E., 2013. Paleo exposure surfaces in Cenomanian – Santonian carbonate reservoirs in the Dezful Embayment, SW IRAN. Journal of Petroleum Geology, 36 (4): 335–362.
Razin, P., Taati, F., van Buchem, FSP., 2010. Sequence stratigraphy of Cenomanian–Turonian carbonate platform margins., Sarvak formation. in the high Zagros, SW Iran: an outcrop reference model for the Arabian Plate. In: van Buchem, FSP., Gerdes, KD., Esteban, M. (eds). Mesozoic and Cenozoic Carbonate Systems of the Mediterranean and the Middle East: Stratigraphic and Diagenetic Reference Models, 329. Geological Society of London Special Publications, pp 187–218.
Reeder, SL., Rankey, EC., 2008. Interactions between tidal flows and oolite shoals, Northern Bahamas. Journal of sedimentary research, 78: 175–186.
Richterd, K., 1983. Calcareous ooids: a synopsis. In: Peryt TM., ed. Coated Grains. Springer-Verlag, Berlin, pp 142–153.
Rigo de Righi, M., Cortesini, A., 1964. Gravity tectonics in foothills structure belt of southeast Turkey. American Association of Petroleum Geologists Bulletin, 48: 1911–1937.
Schlumberger, Ltd. Staff., 1981. Well evaluation conference United Arab Emirates: Qatar, Paris, France, Schlumberger Services Tech. Paris, 271.
Sadooni, FN., 2004. Stratigraphy, depositional setting and reservoir characteristics of Turonian - Campanian carbonates in Central Iraq. Journal of Petroleum Geology, 27(4): 357–371.
Sandberg, PA., 1975. New interpretations of Great Salt Lake ooids and of ancient non-skeletal carbonate mineralogy. Sedimentology, 22: 497–537.
Sandberg, PA., 1983. An oscillating trend in Phanerozoic nonskeletal carbonate mineralogy. Nature, 305: 19–22.
Sandberg, PA., 1985.: Aragonite cements and their occurrence in ancient limestones. In: Schneidermann N, Harris PM., eds. Carbonate cements. Society of Economic Paleontologists and Mineralogists Special Publication, 36: 33–58
Schlanger, SO., 1957. Dolomite growth in coralline algae. Journal of Sedimentary Petrology, 27: 181–186
Schlanger, SO., Jenkyns, HC., Premoli-Silva, I., 1981. Volcanism and vertical tectonics in the Pacific Basin related to global Cretaceous transgressions. Earth and Planetary Science Letters, 52: 435–449.
Scott, RW., Simo, JA., Masse, J-P., 1993. Overview of economic resources in Cretaceous carbonate platforms, In: Simo JA, Scott RW, Asse JP., eds. Cretaceous Carbonate Platforms. American Association of Petroleum Geologists Memoir, 56: 15–24.
Sepehr, M., Cosgrove, JW., 2004. Structural framework of the Zagros Fold–Thrust Belt, Iran. Marine and Petroleum Geology, 21: 829–843
Setudehnia, A., 1972. Iran du Sud-Ouest: Lexique Strat. International Centre National Rechearche Scientifique, Paris, III, Asie, Fasc 9b: 289–376.
Setudehnia, A., 1978. The Mesozoic sequence in southwest Iran and adjacent areas. Journal of Petroleum Geology, 1: 3–42
Sharland, PR., Archer, R., Casey, DM., Davies, RB., Hall, SH., Heward, AP., Horbury, AD., Simmons, MD., 2001. Arabian Plate sequence stratigraphy. GeoArabia Special Publication, 2: 371
Sharp, I., et al., 2010. Stratigraphic architecture and fracture-controlled dolomitization of the Cretaceous Khami and Bangestan Groups: an outcrop case study, Zagros Mountains, Iran. Geological Society London Special Publication, 329: 343–396.
Shearman, DJ., Twyman, J., Zand Karimi, M., 1970. The genesis and diagenesis of oolites. Search Results
Web results, Proceedings of the Geologists' Association, 81: 561–575.
Siewers, FD., 2003. Oolite and coated grains. In: Middleton, GV., Church, MJ., Coniglio, M., Hardie, LA., Longstaffe, FJ., eds. Encyclopedia of Sediments and Sedimentary Rocks. Kluwer Academic Publishers, Dordrecht, Boston and London, pp 502–506.

Simone, L., 1981. Ooids: a review. Earth Science Reviews, 16: 319–355.
Simone, L., Carannante, G., Bassi, D., Cherchi, A., 2012. Rudist-bearing rhodalgal facies in the post-Turonian recovery of peri-Tethyan carbonate systems: a case history from the Nurra region., northwestern Sardinia, Italy.. Geodiversitas, 34(1): 167–187.
Spicer, RA., Corfield, RM., 1992. A review of terrestrial and marine climates in the Cretaceous with implications for modeling the Greenhouse Earth. Geological Magazine, 129: 169– 180.
Stanley, SM., Hardie, LA., 1998. Secular oscillations in the carbonate mineralogy of reef-building and sedimentproducing organisms driven by tectonically forced shifts in sea-water chemistry. Paleogeography, Paleoclimatology, Paleoecology, 144: 3–19.
Sugden, W., Standring, AJ., 1975. Qatar Peninsula: Lexique Strat. International Centre National Rechearche Scientifique, Pads, III, Asie, Fasc 10b3:120 p.
Sumner, D., Grotzinger, JP., 1993. Numerical modeling of ooid size and the problem of Neoproterozoic giant ooids. Journal of Sedimentary Petrology 63(5.:974–982.
Swett, K., Knoll, AH., 1989. Marine pisolites from upper Proterozoic carbonates of east Greenland and Spitzbergen. Sedimentology, 36: 75–93.
Tschopp, RH., 1967a. The general geology of Oman: Proc. 7th World Petroleum Congress, Mexico, 2: 231–242.
Tschopp, RH., 1967b. Development of the Fahud Field, in Origin of oil, geology and geophysics, 7th World Petroleum Congress, Mexico, 2: Amsterdam, Elsevier, pp 243–250.
Tucker, ME., 1984. Calcitic. aragonitic and mixed calcitic- aragonitic ooids from the mid-Proterozoic Belt Supergroup, Montana. Sedimentology, 31: 627–644.
Tucker, ME., 1985. Calcitized aragonite ooids from the Late Precambrian Biri Formation of Southern Norway. Sedimentary Geology, 43: 67–84.
Tucker, ME., Wright, VP., 1990. Carbonate Sedimentology. Blackwell Scientific Publications, Oxford.
Vail, PR., Mitchum, JRRM., Todd, RG., Vidmier, JM., Thompson, S., Sangree, JB., Buaa, JW., Hatleid, WG., 1977. Seismic Stratigraphy-Application to Hydrocarbon Exploration. American Association of Petroleum Geologists Memoir, 26.
van Buchem, FSP et al., 2010. Regional stratigraphic architecture and reservoir types of the Oligo-Miocene deposits in the Dezful Embayment., Asmari and Pabdeh Formations. SW Iran. Geological Society of London Special Publication, 329: 219–263.
van Buchem, FSP., Simmons, MD., Droste, HJ., Davies, RB., 2011. Late Aptian to Turonian stratigraphy of the eastern Arabian Plate–depositional sequences and lithostratigraphic nomenclature. Petroleum Geoscience, 17(3): 211–222.
Veizer, J., 1977. Diagenesis of pre-Quaternary carbonates as indicated by tracer studies. Journal of Sedimentary Petrology, 47: 565–581
Veizer, J., Demovic, R., 1973. Environmental and climatic controlled fractionation of elements in the mesozoic carbonate sequences of the Western Carpathians. Journal of Sedimentary Petrology, 43(1): 258–271.
Veizer, J., Hoefs, J., 1976. The nature of O18/O16 and C13/C12 secular trends in sedimentary carbonate rocks. Geochimica et Cosmochimica Acta, 40: 1387–1395.
Veizer, J et al., 1999. 87Sr/86Sr, 13C and 18O evolution of Phanerozoic seawater. Chemical Geology, 161: 59–88.
Videtich, PE., McLimans, RK., Watson, HKS., Nag, RM., 1988. Depositional, diagenetic, thermal and maturation histories of Cretaceous Mishrif Formation, Fateh Field, Dubai. American Association of Petroleum Geologists Bulletin, 72: 1143–1159.
Wilkinson, BH., Buczynski, C., Owen, RM., 1983. Chemical control on carbonate phases: implications from Upper Pennsylvanian calcite-aragonite ooids of southeastern Kansas. Journal of Sedimentary Petrology, 54(3): 932–947.
Wilkinson, BH., Buczinski, C., Owen, RM., 1984. Chemical control of carbonate phases: implications from Upper Pennsylvanian calcite-aragonite ooids of Southeastern Kansas. Journal of Sedimentary Petrology, 54: 932–947.
Wilkinson, BH., Owen, RM., Carrol, AR., 1985. Submarine hydrothermal weathering, global eustasy andcarbonate polymorphism in Phanerozoic marine oolites. Journal of Sedimentary Petrology, 55: 171–183.
Wilson, JL., 1975. Carbonate facies in geologic history. Springer, New York.
Wilson, HH., 1969. Late Cretaceous eugeosynclinal sedimentation gravity tectonics and ophiolite emplacement in Oman Mountains, southeast Arabia. American Association of Petroleum Geologists Bulletin, 53: 626–671.
http://paleoportal.org/index.php?globalnav=time_space&sectionnav=period&period_id=18